Biochimica et Biophysica Acta 1793 (2009) 1876–1885

Contents lists available at ScienceDirect

Biochimica et Biophysica Acta

journal homepage: www.elsevier.com/locate/bbamcr

NOA36/ZNF330 is a conserved cystein-rich protein with proapoptotic activity in human cells

Ivan S. de Melo [a], Concepción Iglesias [a], Alicia Benítez-Rondán [b], Francisco Medina [b], Juan Pedro Martínez-Barberá [c], Jorge Bolívar [a,*]

[a] Departamento de Biomedicina, Biotecnología y Salud Pública, Facultad de Ciencias, Universidad de Cádiz, 1150 Puerto Real, Spain
[b] Unidad de Investigación Hospital Universitario Puerta del Mar, 11009 Cádiz, Spain
[c] Neural Development Unit, Institute of Child Health, 30 Guilford Street, WC1N 1EH London, UK

ARTICLE INFO

Article history:
Received 19 June 2009
Received in revised form 26 October 2009
Accepted 28 October 2009
Available online 4 November 2009

Keywords:
Apoptosis
NOA36
ZNF330
Etoposide
Camptothecin
Mitochondria

ABSTRACT

Translocations of regulator proteins from or to the mitochondria are key events in apoptosis regulation. NOA36/ZNF330 is a highly evolutionary conserved protein with a characteristic cystein-rich domain. In this work we address its mitochondrial localization and we demonstrate that a blockage of endogenous NOA36/ZNF330 expression by small-interfering RNA (siRNA) reduced apoptotic response to etoposide (ETO), camptothecin (CPT) and staurosporine (STS) but not to CH11 anti-Fas antibody or tumour-necrosis-factor-related apoptosis-inducing ligand (TRAIL) in HeLa cells. In contrast, when ectopically expressed in the cytoplasm, NOA36/ZNF330 induces apoptotic cell death. We also found that the domain responsible for this proapoptotic activity is located its cystein-rich region. We propose that NOA36/ZNF330 is translocated from the mitochondria to the cytoplasm when apoptosis is induced and that it contributes to cytochrome *c* release.

1. Introduction

Apoptosis or selective cell suicide is a crucial process required for normal embryo development, maintenance of tissue homeostasis and for proper function of the immune system [1]. A deficient regulation of this process underlies many diseases; for example, failure of cells to initiate apoptosis in response to DNA damage has been implicated in the development and progression of cancer [2,3], whereas inappropriate activation of apoptosis is thought to be a contributing factor in Alzheimer's and Parkinson's diseases [4,5]. Apoptosis is triggered by a cascade of proteolytic activation of caspase proteases that eventually ends in the digestion of cell proteins, nuclear DNA degradation, and cell death [6].

The molecular machinery for caspases activation can be induced by two main pathways: the "death receptors pathway," activated by extracellular signals and mediated by caspase-8 [7,8] and the "intrinsic pathway," which is induced by several intracellular stress conditions. The mitochondrion is a key organelle in the regulation of the latest [9] and many regulators like the antiapoptotic proteins of the Bcl-2 family, including Bcl-2 and Bcl-X_L, are permanently located at the mitochondria and preserve mitochondrial integrity [10]. However migration of regulatory molecules from or to the mitochondria is a frequent feature in apoptosis regulation. For example, some proapoptotic members of this family such as Bax [11] and the BH3-only proteins Bad [12], Bid [13], Bim [14] or Bmf [15] move from other cellular compartments to the mitochondria in response to apoptotic stimuli. These events result in mitochondrial pore formation and the release of cytochrome *c* from the mitochondria into the cytosol [16–18], where it binds to Apaf1 to form an oligomeric assembly called "apoptosome," which recruits and activates caspase-9 and allows the activation of effectors caspases such as caspase-3 [19]. Cytochrome *c* is not the only protein released from mitochondria during apoptosis, for instance Smac-Diablo [20,21], HtrA2/Omi [22,23] and ARTS [24] are mitochondrial proteins liberated into the cytosol when cells undergo apoptosis, while AIF [25] and Endonuclease G [26,27] are also normally confined to the mitochondria but they translocate to the nucleus when apoptosis is induced. Once they are released from the mitochondria, all these proteins actively promote apoptotic cell death.

Molecular studies of many human autoantigens have demonstrated the important function of these proteins and have revealed new cellular mechanisms [28]. In this work we investigate the subcellular localization and function of NOA36 (*N*ucleolar Autoantigen-36 kDa) also named ZNF330. This is a protein highly preserved during the evolution that was previously described as a nucleolar autoantigen. NOA36 is widely distributed in human tissues with significantly higher expression levels in heart and skeletal muscle [29]. The human NOA36 gene was mapped by FISH to chromosome 4q31.1 q31.2 and is comprised of 10 exons and spans 16 kb of genomic DNA [30]. In spite

* Corresponding author. Departamento de Biomedicina, Biotecnología y Salud Pública, Facultad de Ciencias, Polígono Rio San Pedro s/n, 11510 Cádiz, Spain. Tel.: +34 956 01 63 91; fax: +34 956 01 62 88.
E-mail address: jorge.bolivar@uca.es (J. Bolívar).

0167-4889/$ – see front matter © 2009 Elsevier B.V. All rights reserved.
doi:10.1016/j.bbamcr.2009.10.011

its high grade of homology throughout distant phyla, no function, either at cell or at organism level, has been associated to NOA36 so far. Interestingly NOA36 was identified as a tyrosine kinase target in Jurkat cells in a recent proteomic study designed to detect tyrosine kinases substrates [31].

Here we show that NOA36 normally localizes at the mitochondria in mammalian cells and that knockdown of NOA36 by RNAi reduces the apoptotic response to ETO, CPT and STS but not to the death receptor ligands anti-Fas antibody and TRAIL. We also show that NOA36 is translocated from the mitochondria into cytoplasm when apoptosis is triggered. Furthermore, when ectopically expressed in the cytoplasm, NOA36 induces cytochrome *c* release and caspase-3 activation. This apoptotic phenotype is reverted by over-expression of Bcl-2 and Bcl-X_L. These results suggest that NOA36 is a mediator of the mitochondrial apoptotic pathway.

2. Materials and methods

2.1. Cell lines, culture conditions, drugs treatments and transfections

HeLa and CHO were cultured in Dulbecco's modified Eagle's medium supplemented with 10% foetal bovine serum and 100 U/ml penicillin and 100 μg/ml streptomycin at 37 °C in a CO_2 incubator. For drugs treatments, HeLa cells were exposed to ETO (from SIGMA) (25 μM for 48 h), CPT (from SIGMA) (20 μM for 48 h), STS (from SIGMA) (0.25 μM for 5 h), TRAIL (from Peprotech) (100 ng ml^{-1} for 5 h) or anti-Fas antibody (CH11 clone) (from Beckman Coulter) (250 ng ml^{-1} for 5 h). Transient transfection of HeLa cells were performed using 6 μl of jetPEI (Polyplus), and 1.8 μg of plasmid in 35 mm plates, according to the manufacturer's instructions. Cells were plated 24 h before transfections.

2.2. Subcellular fractionation and proteinase K digestion

Approximately 5×10^6 cells were seeded per 100-mm dish. On the next day, cells were scraped and washed once with ice-cold phosphate-buffered saline pH 7.4 (PBS). Low salt homogenization buffer (LS-HB) containing 10 mM TRIS, pH 6.7, 10 mM KCl, 0.15 mM $MgCl_2$ was added (600 μl of LS-HB/dish) and left 10 min on ice. The cells were homogenized by 30 strokes with a Dounce homogenizer and by passing 15 times through an 18-G needle and then sucrose was added to a final concentration of 0.25 M. The homogenate was centrifuged twice at 1500 *g* for 3 min at 4 °C. The pellet represented the nuclear fraction. The supernatant was centrifuged at 5000 *g* at 4 °C for 10 min, resulting in the mitochondria fractions (pellet). The supernatant was centrifuged at 100,000 *g* for 1 h at 4 °C to collect the cytosolic fraction (supernatant). The cytosolic supernatant and the mitochondrial and nuclear pellets were fractionated on SDS-PAGE for subsequent immunoblot analysis. For proteinase K partial digestions, mitochondria pellets were resuspended in 60 μl of PBS pH 7.4 and incubated with proteinase K (5 μg/ml) for 5 min, then 1 mM PMSF was added and the mitochondria were pelleted, dissolved in sample buffer and resolved by SDS-PAGE.

2.3. Immunostaining

For indirect immunofluorescence staining, cells grown on coverslips were washed with PBS and fixed in cold acetone for 10 min at

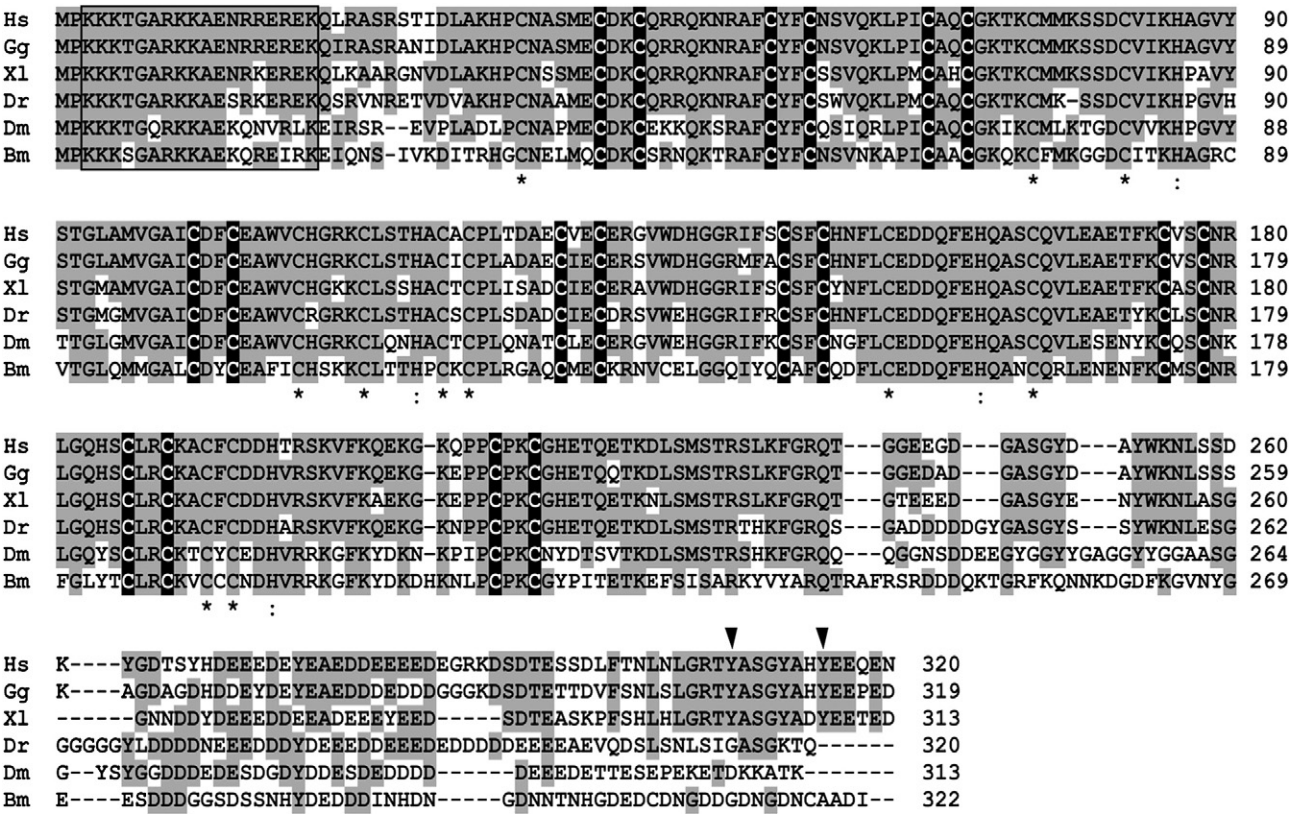

Fig. 1. ClustalW alignment of NOA36 amino acids sequences in species from different phyla. Species are indicated by the following abbreviations from top to bottom: mammal *Homo sapiens* (Hs), avian *Gallus Gallus* (Gg), amphibian *Xenopus laevis* (Xl), fish *Danio rerio* (Dr), insect *Drosophila melanogaster* (Dm) and the filarial nematode *Brugia malayi* (Bm). Conserved amino acids in at least three species are shaded in grey. A putative bipartite nuclear localization signal is boxed at the amino terminal. The conserved CXXC motifs are indicated in white on black background. Other conserved cysteine (asterisk) and histidine (two dots) residues in all the sequences are indicated. Note the high proportion of acidic amino acids (D and E) in the polyacidic carboxyl terminal domain (from amino acids 260 to 320 in the human protein). Phosphorylated Tyr residues in Jurkat cells are indicated with two arrowheads.

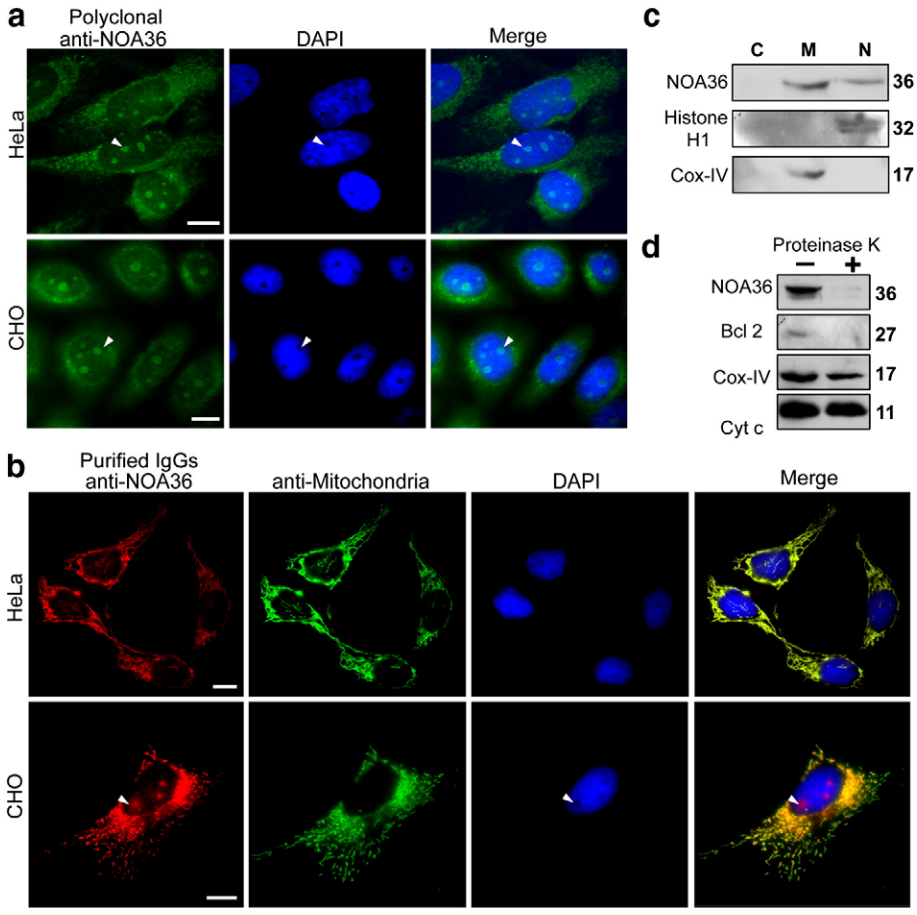

Fig. 2. NOA36 is localized at the nucleoli and the mitochondria of mammalian cells at interphase. (a) Immunofluorescence analysis on HeLa and CHO cells using a crude polyclonal serum. In green, NOA36 immunodetection; in blue, DAPI chromatin staining. Nucleoli are indicated with arrowheads. The merged images show NOA36 and nucleoli colocalization. (b) Immunofluorescence analysis on HeLa and CHO cells using affinity-purified NOA36 IgGs. In red, NOA36 immunodetection. In green, ATP synthase immunodetection, showing mitochondria staining. In blue, DAPI chromatin staining, in which nucleoli can be appreciated (arrowhead). Merged image of the triple fluorescent labeling shows co-localization of NOA36 and the mitochondrial marker. Note that nucleolar staining is visible in CHO (arrowheads) but not in HeLa cells, probably due to a lower accumulation of NOA36 in HeLa nucleoli. Bars, 10 μm. (c) Immunoblot analysis reveals NOA36 retention in mitochondrial and nuclear fractions. Protein extracts were divided into cytosol (lane C), mitochondrial (lane M) and nuclear (lane N) fractions and analysed by Western blot using affinity-purified anti-NOA36 IgGs. The quality of the fractionation is verified by controlling the distribution of specific subcellular markers (COX-IV as mitochondria specific marker, and histone H1 as nuclear specific marker). (d) Partial proteinase K treatment indicates that NOA36 is located on the outside of the outer mitochondrial membrane. Bcl-2 is located in the external membrane, cytochrome *c*, located in the intermembrane space and COX-IV complex, in the inner mitochondrial.

−20 °C (anti-NOA36 and anti-Flag antibodies) or 4% paraformaldehyde before permeabilization with 0.1% Triton X-100 (anti-active caspase-3, anti-cytochrome *c* and anti-ATP synthase antibodies). Cells were then washed with PBS and incubated with primary antibodies diluted in PBS (1:10 of immunoaffinity-purified anti-NOA36 IgGs; 1:100 of anti-ATP synthase-subunit-α 7H10 (Molecular Probes); 1:500 of anti-Flag M2 (SIGMA); 1:1000 of anti-active caspase-3 (SIGMA) and 1:80 of anti-cytochrome *c*, clone 6H2B4, from AbCam) at 37 °C for 45 min. Cells were then washed with PBS for 30 min at room temperature and incubated with Alexa fluor 488 or 555-labeled secondary antibodies (Molecular Probes) at 37 °C for 45 min. Finally, cells were washed twice in PBS and mounted in PBS-glycerol containing DAPI at 0.1 μg/ml. A Zeiss Axiophot microscope equipped with a 63× NA 1.3 oil immersion objective was routinely used. Images were taken using a SPOT Camera (Diagnostic Instruments Inc.) and processed using Adobe Photoshop software.

2.4. Western blot analysis

Protein lysates from total cell extracts and subcellular fractions from HeLa cells were separated on 15% SDS-polyacrylamide gels, electrophoretically transferred to Nitrocellulose membranes

Fig. 3. Downregulation of NOA36 desensitizes cells to ETO, CPT and STS-mediated apoptosis and NOA36 is translocated to cytosol during apoptosis. (a) siRNA-mediated knockdown of NOA36. Western blot analysis of NOA36 expression in HeLa cells transfected with an equimolecular mix of two different siRNAs against NOA36 or with control siRNA against EGFP. NOA36 expression in non transfected cells is also shown (lane C). (b) Knockdown of endogeneous NOA36 protects against CPT, ETO and STS-induced apoptosis but not against TRAIL or anti-Fas antibody treatments. HeLa cells were transfected with NOA36 siRNAs or EGFP siRNA (control) then grown in the presence or in the absence of CPT, ETO, STS, TRAIL and anti-Fas antibody. Apoptotic cells were analysed by FACS using an antibody against the active form of caspase-3. FACS histograms plots from representative experiments are shown, where M1 gates active caspase-3 positive cells respect to untreated cells (diagram not shown). Graph represents the average of the percentage of caspase-3 active cells ($n=3$). Error bars are standard deviation of the mean. On the right of each diagram, a profile of caspase-3 activation (C-3) in the different conditions is illustrated by Western blot. Levels of NOA36 (N) and α-tubulin (α-T) are also shown for each experiment. Significant differences ($P<0.05$) are marked by asterisks (*). (c) Immunoblot analysis of cytosolic and mitocondrial NOA36 in normal control cells (lane C) and ETO (lane ETO) and TRAIL (lane TRAIL) treated HeLa cells. On the right, a diagram showing the quantification of mitochondrial NOA36 in control, ETO and TRAIL treated cells. Immunoblots from three different experiments were analysed. The mitochondrial loading marker COX-IV of the same sample was used to normalize. Significant differences ($P<0.05$) are marked by asterisks (*). (d) Immunolocalization of NOA36 (green) in non-treated (NTC) and CPT, ETO, STS and TRAIL treated HeLa cells. In red, mitochondrial marker (anti-ATP-synthase). In blue, DAPI to label chromatin. Merge image of the triple labeling is shown. In non-treated and CPT HeLa cells NOA36 localizes at the mitochondria. However, cells treated with CTP, ETO and STS and TRAIL show a NOA36 diffuse cytoplasmic staining. Bars, 10 μm.

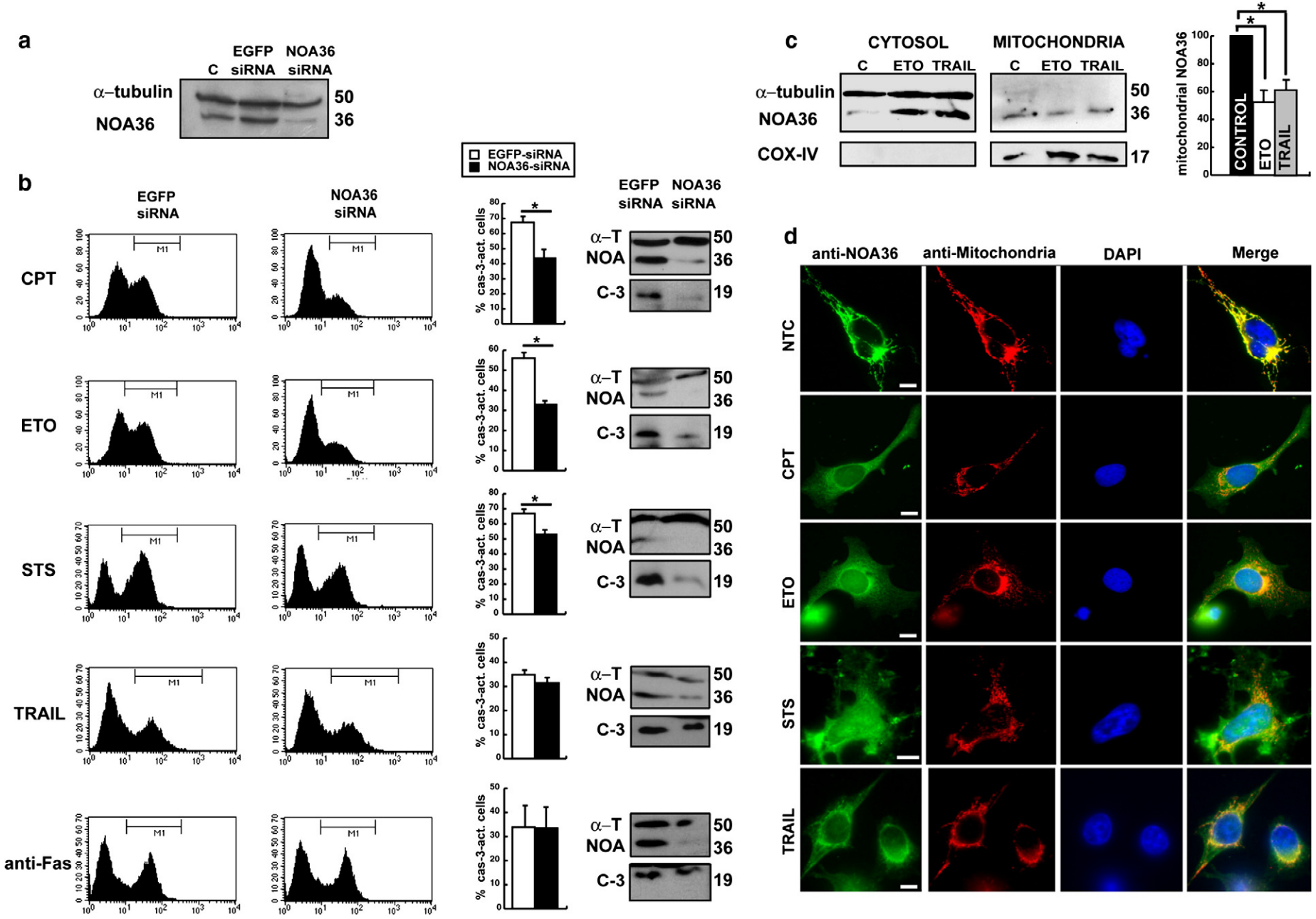
a
C
EGFP siRNA
NOA36 siRNA
α–tubulin
NOA36
50
36
b
EGFP siRNA
NOA36 siRNA
CPT
ETO
STS
TRAIL
anti-Fas
M1
EGFP-siRNA
NOA36-siRNA
% cas-3-act. cells
α–T
NOA
C-3
50
36
19
c
CYTOSOL
MITOCHONDRIA
C
ETO
TRAIL
α–tubulin
NOA36
COX-IV
50
36
17
mitochondrial NOA36
CONTROL
ETO
TRAIL
d
anti-NOA36
anti-Mitochondria
DAPI
Merge
NTC
CPT
ETO
STS
TRAIL

(Millipore) and subjected to immunoblot analysis with anti-NOA36 IgGs (1:1000), anti-COX IV (1:1000 dilution of 20E8 from AbCam), anti-histone H1 (1:100 of monoclonal 12C7, a gift of M.M. Valdivia), anti-cytochrome *c* (1:3000 of 7H8 from Santa Cruz Biotechnology) anti-α-—tubulin (1:3000 of DM1A from SIGMA) anti-active caspase-3 (1:500 of Asp175 from Cell Signalling) and anti-Bcl-2 (1:600 of C-2 5 from Santa Cruz Biotechnology). Following incubation of the membranes with HRP-coupled secondary antibodies (SIGMA), proteins were visualised by ECL detection kit (Roche). For Western blot quantification of NOA36 the software GeneTools (Syngene) was used.

2.5. Plasmids and constructs

Mammalian expression cytomegalovirus promoter-based vector constructs encoding C-terminal tagged Flag-NOA36 (Invitrogen), N-terminal tagged NOA36-EGFP (Clontech) and NOA36-Cherry (a gift of Dr. R.Y. Tsien) were generated by PCR amplification from the human full-length NOA36 cDNA [29]. PCR products incorporated EcoRI site on the 5′ end and the BamHI site on the 3′ end. Eight truncanted fusion proteins containing amino acids 1–33, 40–320, 40–239, 33–85, 92–139, 136–185, 178–239, 218–320 of NOA36 were expressed as fusion proteins to EGFP. All constructs were sequenced. GFP-Bcl-2 and GFP-Bcl-X_L constructs are gifts from Dr. R. J. Youle.

2.6. Knockdown of endogenous NOA36 by siRNA and apoptosis quantification by FACS

Sense and anti-sense oligonucleotides corresponding to the following cDNA sequences were purchased from SIGMA for NOA36: CACUCAUGUCUCCGUUGU AdTdT (nucleotides 723–741) and UUAGCU AAACAUCCAUGUAdTdT (nucleotides 1032–1050). HeLa cells were transfected with Interferin (Polyplus) according to the manufacturer's protocol in the presence of NOA36 siRNA or EGFP siRNA (GCA AGC UGA CCC UGA AGU UCA U) as a control. Cells were scraped 72 h after transfection and protein extracts were immunobloted to evaluate knockdown of endogenous NOA36 or kept in culture in the presence or in the absence of ETO, CPT, STS, TRAIL or anti-Fas antibody. Then, were detached by trypsin-EDTA treatment, washed in PBS and fixed in 4% paraformaldehide (500 μl, 15 min, RT). After an additional washing, permeabilization and staining with phycoerytrin-conjugated rabbit polyclonal antibody against active caspase-3 (Becton Dickinson) were performed in the same step (100 μl 0.2% triton X-100, 1/20 antibody dilution, 30 min, RT, in the dark). Finally cells were washed again and acquired in a FACScalibur flow cytometer (Becton Dickinson). Cells were gated on a forward/side scatter plot and analyzed for active caspase-3 expression with CellQuest software (Becton Dickinson).

2.7. Cell death analysis by epifluorescence in transfected cells

1×10^6 transfected HeLa cells seeded onto coverslips were grown for 24–48 h before being fixed in 4% paraformaldehyde–PBS for 20 min at room temperature, then permeabilised in 0.1% Triton X-100 and stained with 2-(4-amidinophenyl)-1H-indole-6-carboxamidine (DAPI) (SIGMA), at room temperature for 2 min. Coverslips were then mounted in PBS–glycerol for EGFP fluorescence observation or subjected to immunostaining with an anti-Flag antibody (SIGMA). Approximately 400 transfected cells were counted for each

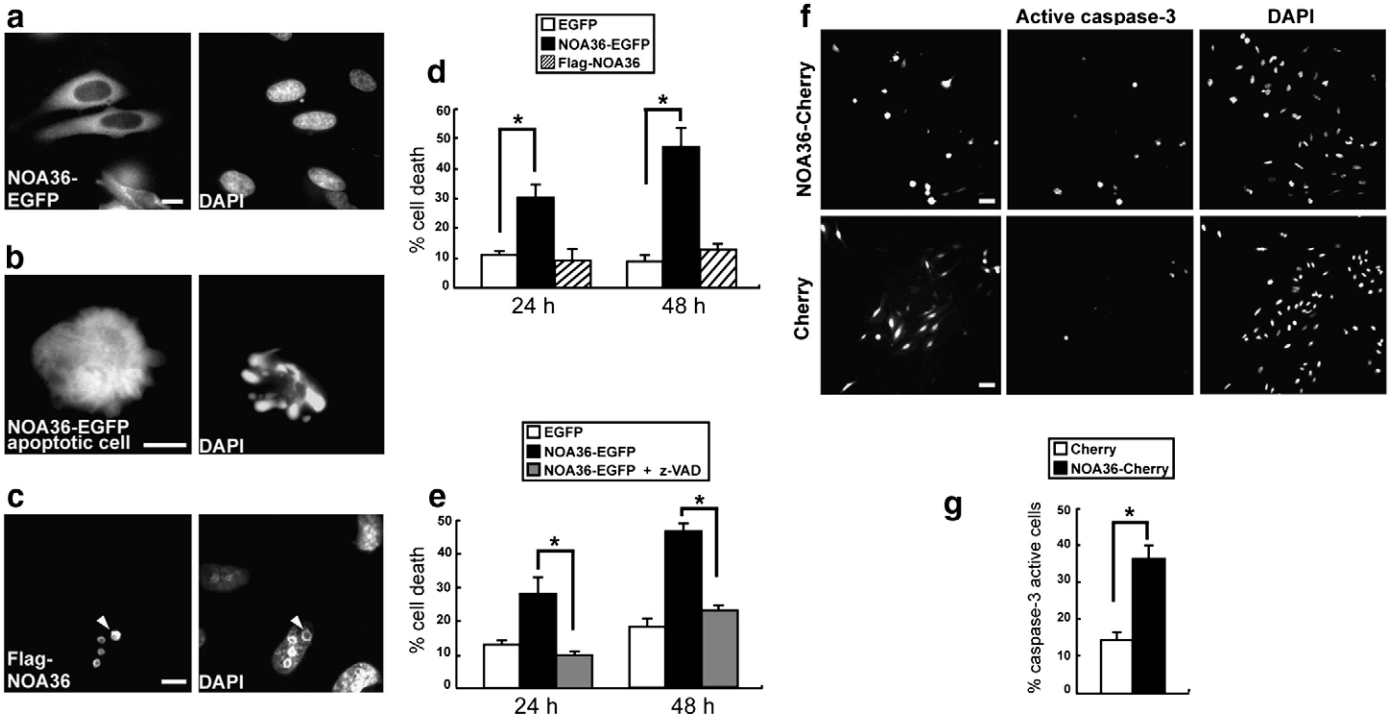

Fig. 4. NOA36 cytoplasmic ectopic expression induces apoptotic cell death in HeLa cells. (a) NOA36-EGFP is located in the cytoplasm. On the left panel, transient transfection assay with NOA36-EGFP. DAPI staining is shown to visualize nuclei. (b) Transfected cell showing signs of apoptosis. Note the condensed/fragmented chromatin and the membrane blebbing, characteristic features of apoptotic cell death. (c) Transient trasfection assay of a Flag-NOA36 expressing vector on HeLa cells. On the left, Flag-NOA36 and on the right panel, DAPI staining to visualize nuclei. Flag-NOA36 tagged protein is located in the nucleoli (arrowheads). Bars, 10 μm. (d) Quantification of the cell death rate induced by either cytoplasmic NOA36-EGFP (black bar), nucleolar Flag-NOA36 (striped bar) or control empty pEGFP vector (white bar) at 24 and 48 h post-transfection. (e) z-VAD-fmk pan-caspase inhibitor reduces the rate of cellular death in cells expressing cytoplasmic NOA36-EGFP. The graphic shows the death rate in transfected cells with pEGFP control vector (white bar) and NOA36-EGFP transfectants grown in a normal medium (black bar) or in 100 μM z-VAD-fmk supplemented medium (grey bar). Cells were monitored 24 and 48 h after transfection. (f) NOA36 cytoplasmic expression induces caspase-3 activation. On the left, NOA-cherry transfected cells (upper panels) and cherry empty vector (lower panels) are labeled with an antibody that specifically recognizes the active form of the caspase-3 (central panels). DAPI staining is also shown to visualize cells nuclei. Bars, 100 μm. (g) Quantification of active caspase-3 positive cells in NOA36-Cherry (black bar) and in Cherry (white bar) transfected cells 48 h after transfection. The error bars in (d), (e) and (g) represent standard deviation of the mean. Significant differences ($n=4$, $P<0.05$) are marked by asterisks (*).

experiment ($n \geq 3$) from random fields under the fluorescence microscope. Apoptotic cells were distinguished based on morphological alteration typical of adherent cells undergoing apoptosis (becoming rounded, having blebbing cytoplasm, and condensed chromatin) or by immunofluorescence with an antibody to the active caspase-3 or with an antibody to cytochrome *c*. For analysis of caspase inhibition, cells were treated with 100 μM z-VAD-FMK (SIGMA) 8 and 24 h after transfection.

2.8. Statistics

Comparisons between groups were performed with Student's *t*-test for paired samples (two-tailed) ($n \geq 3$) and significant differences ($p < 0{,}05$) were denoted by an asterisk.

3. Results

3.1. NOA36 is a highly evolutionary conserved protein

Since the first cDNA encoding NOA36 sequence was published [29], many EST and genome projects have been completed, which allowed us to perform a more thorough analysis of the degree of conservation of NOA36 during evolution. ClustalW alignment of NOA36 protein sequences from different phyla allows now a better understanding of the primary structure of this protein (Fig. 1). Besides a very similar number of amino acids (from 313 to 322), three different domains can be deduced in NOA36 protein. At both ends two characteristic sequences can be predicted: a putative amino-terminal nuclear localization signal and a poly-acidic region, with a 42% of Asp and Glu residues in the last 60 amino acid carboxyl-terminal in the human protein. However, the most characteristic feature of this protein is a Cys-rich domain that consists of 214–216 amino acids with at least 16% of Cys residues. The 29 Cys in the human protein are arranged in the same relative position in all available orthologous sequences, with nine Cys-X-X-Cys highly conserved motifs indicative of several putative zinc fingers. These motifs make NOA36 a potential Zn finger protein with at least four Zn binding motifs. The striking grade of homology throughout distant phyla of NOA36 proteins prompted us to investigate this protein whose molecular function was unknown.

3.2. NOA36 protein is associated with the mitochondria and the nucleolus

NOA36 was identified a decade ago as a nucleolar autoantigen in a patient suffering from rheumatoid arthritis and its subcellular localization was determined by indirect immunofluorescence with a specific polyclonal serum raised against the recombinant hamster NOA36 [29]. These experiments demonstrated that NOA36 was located predominantly but not exclusively at the nucleolus, with some diffuse/punctuate cytoplasmic staining, in several mammalian cell lines (Fig. 2a). Our first aim was to investigate whether the cytoplasmic staining of this polyclonal serum was genuine NOA36 localization. To address this point we affinity purified specific anti-NOA36 immunoglobulins (IgGs) using the human NOA36 recombinant protein immobilized on sepharose beads. Immunofluorescence assays using the purified anti-NOA36 IgGs showed a pattern that colocalized with a mitochondrial marker in mammalian cells (Fig. 2b). Although NOA36 could be detected at the nucleoli in CHO cells, no nucleolar staining could be observed in HeLa, probably due to a lower nucleolar NOA36 concentration in this cell line. Later obtained polyclonal serum to NOA36 recombinant protein confirmed its mitochondrial localization (data not shown). Western blot assay with the affinity purified IgGs corroborated the mitochondrial and nuclear NOA36 localization (Fig. 2c). In order to determine if NOA36 is located within the mitochondria or associated with the outer membrane of this organelle, we subjected a mitochondria extract to limited proteinase K treatment, which results in digestion of proteins located on the mitochondria cytosolic surface. This experiment clearly demonstrated that NOA36 was digested by proteinase K, as occurs with Bcl-2, a protein that is associated to the external membrane (Fig. 2d). However, cytochrome *c*, which is located at the intermembrane space and the COX IV complex, which is embedded in the inner mitochondrial membrane, were resistant to proteolysis under proteinase K digestion, indicating that the mitochondrial external membrane remained intact throughout the experiment. We therefore conclude that NOA36 is a mitochondrial protein very likely associated with the outer layer of the external mitochondrial membrane.

3.3. NOA36 downregulation reduces sensitivity to etoposide, camptothecin, and staurosporine but not to anti-Fas antibody or TRAIL

Because mitochondria play a key part in the regulation of apoptosis we analyzed whether loss of function of NOA36 had any effect in this process by suppressing expression of endogenous NOA36 by siRNA in HeLa cells. After Western blot analysis we found that an equimolecular mix of two NOA36 siRNAs brought about a strong inhibition of NOA36 expression whereas control siRNA against GFP had no effect (Fig. 3a and Fig. 1 SM). To study a possible role of NOA36 in apoptosis, we used ETO, CPT and STS as intrinsic pathway inducers and anti-Fas antibody and TRAIL as death receptor ligands. We then analyzed apoptosis by fluorescence-activated cell sorting (FACS) with an antibody to the active form of caspase-3, one the main apoptosis effectors. We found reduced active-caspase-3 staining respect to control siRNA for ETO, CTP and, in a lower extent, for STS treatments ($P < 0.05$) but not for anti-FAS antibody or TRAIL exposure. Coherently with FACS analysis, a diminution of caspase-3 activity was detected in Western blot analysis of NOA36 siRNA treated cells in the ETO, CPT and STS, but not after anti-Fas or TRAIL treatments (Fig. 3b). These data together with NOA36 mitochondrial localization suggest a proapoptotic role of NOA36 in the regulation of the mitochondrial apoptotic pathway.

3.4. NOA36 migrates to cytoplasm during apoptosis

To study whether NOA36 mitochondrial localization is altered in cells undergoing apoptosis, we analyzed the localization of NOA36 by Western blot assays in cytosolic and mitochondrial extracts in HeLa cells. NOA36 can be detected in the cytosolic fraction in the ETO and TRAIL treated cells, but it is barely detectable in the cytosol of normal control cells. On the other hand, quantification by Western blottings of mitochondrial NOA36 by normalizing with COX-IV mitochondrial marker showed that NOA36 levels are 50% lower in ETO and 40% lower in TRAIL than in non-treated control cells (Fig. 3c). This translocation can be visualized by immunofluorescence assays. Upon apoptosis induction with ETO, CPT, STS and in a less extent in TRAIL, NOA36 staining changed from a filamentous mitochondrial pattern to a more diffuse cytoplasmic distribution whereas the mitochondrial marker (ATP-synthase-subunit-α) still showed a mitochondrial pattern (Fig. 3d).

3.5. Ectopic localization of NOA36 in the cytoplasm induces a high rate of apoptotic cell death

We next asked whether NOA36 cytoplasmic localization might have an active role in cell death or if it was just a consequence of the mitochondrial disruption caused by apoptosis. To this end, we investigated the effect of cytoplasmic NOA36 on cell survival by using the fusion protein NOA36-EGFP. Transient transfection assays of NOA36-EGFP in HeLa cells showed a cytoplasmic, but not nucleolar or mitochondrial distribution (Fig. 4a). We also found the same

cytoplasmic distribution when NOA36 was fused to the C-terminal of EGFP (data not shown). It has been shown that expression of native proteins fused to tag sequences or fluorescence proteins, may impair normal cellular localization of the fusion protein compared with the endogenous form. This feature has previously been used to study the effect of proapoptotic proteins when ectopically expressed in other cellular compartments [32]. Transfected cells were monitored for NOA36-EGFP ectopic expression and for nuclear chromatin condensation by DAPI staining (Fig. 4b). We observed that NOA36-EGFP cytoplasmic localization induced around 30% and 50% of cell death in transfected cells at 24 and 48 h after transfection, respectively (Fig. 4d), but apoptosis rate reach 91.5% at 96 h after transfection (Fig. 2 SM). On the other hand, the quantification of apoptosis in fixed cells could underestimate the rate of apoptosis due to the fact that HeLa terminal apoptotic cells can be detached from coverslip (Fig. 2 SM). It has been described that EGFP may aggregate within cells, which may have a toxic effect. To check that cell death was specifically being caused by NOA36, and not due to EGFP aggregates, we carried out similar experiments using the red monomeric fluorescent protein Cherry, which does not to aggregate upon transfection [33]. Fusion protein NOA36-Cherry also localized to the cytoplasm in HeLa cells and leaded to a similar cell death rate when compared to NOA36-EGFP (data not shown). To further confirm that apoptosis was the cause of cell death, we treated NOA36-EGFP transfectans with the cell permeable pan-caspase inhibitor z-VAD-fmk [34] and monitored cell death as previously described. As shown in Fig. 4e, this treatment reduced significantly the cell death rate ($P<0.05$) to a level similar to that observed in cells expressing EGFP alone.

We next investigated the relationship between NOA36 apoptotic induction and caspase-3 activation by fluorescence microscopy with an antibody against the active form of caspase-3 (Fig. 4f). We detected that $36\pm4\%$ of the NOA36-Cherry transfected cells were active caspase-3 positive at 48 h after transfection versus $14\pm2\%$ in cells transfected with the empty vector ($P<0.05$) (Fig. 4g).

Since native NOA36 is also localized in the nucleolus, we monitored the cell death rate in cells expressing the tagged protein Flag-NOA36. Flag-NOA36 is located at the nucleoli in most of the transfected cells (Fig. 4c). In this case, cell death was not induced upon transfection of Flag-NOA36 when compared with cells transfected with the control plasmid (Fig. 4d). Overall, these data suggest that cytoplasmic localization of NOA36 is not just an irrelevant consequence of mitochondrial disruption during apoptosis; on the contrary it is sufficient to induce cell death.

4.6. The NOA36 cell death domain is located within the NOA36 cystein-rich region

To identify the NOA36 domain that induced cell death, several truncated NOA36-EGFP constructs were analyzed in transient transfection assays by monitoring condensed chromatin as an indicator of cell death. These studies indicated that, out of the 3 putative domains of the protein, only the cysteine-rich domain consistently induced apoptosis. Truncated NOA36 proteins lacking the N-terminal nuclear localization signal and/or polyacidic C-terminal induced an even a higher cell death rate than the full length protein (Fig. 5a). Moreover, overexpression of several non-overlapping truncated NOA36 proteins within the cystein-rich domain, fused to EGFP was used to determine which part of this domain was sufficient to induce apoptosis (Fig. 5b). We found that only a putative zinc finger domain between amino acids 92–139 could significantly induce apoptosis respect to the empty vector in percentage similar to that caused by the full-length protein ($P<0.05$). We can therefore conclude that this sequence is the main responsible for the cell death caused by NOA36.

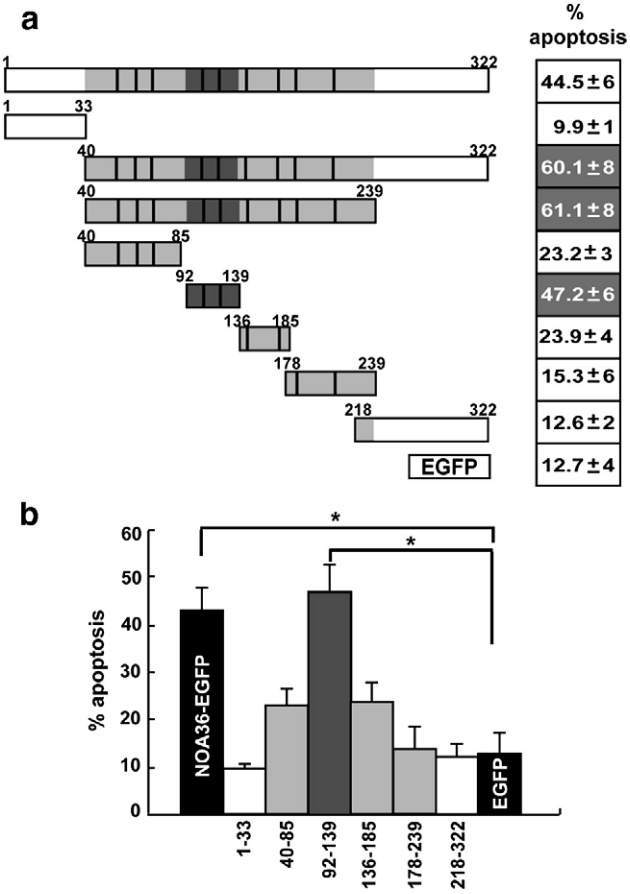

Fig. 5. Mapping of the domain responsible for NOA36 cell death induction. (a) Schematic representation of the different constructs used for the mapping of NOA36 cell death domain. Cell death rate caused by these constructs at 48 h after transfection are indicated at the right ($n=3$). Significant differences ($P<0.05$) respect to the empty vector (EGFP) are marked in white on grey background. All constructs represented are C terminal fusion proteins to EGFP. In light grey the Cys rich domain (black bars represent CXXC motives). The zinc finger domain responsible for the strongest cell death induction (residues 92–139) is highlighted in dark grey. (b) Bar diagram showing cell death rates induced by non-overlapping truncated proteins. The error bars represent standard deviation of the mean. Significant differences ($n=3$, $P<0.05$) are marked by asterisks (*).

3.7. Apoptosis induced via NOA36 cytoplasmic expression is mediated by cytochrome c release and is inhibited by Bcl-X_L and Bcl-2

We subsequently asked whether NOA36 could activate caspase-3 via mitochondrial membrane permeabilization and cytochrome *c* release, a decisive event of the intrinsic pathway of apoptosis. We studied the fate of cytochrome *c* in NOA36-EGFP and EGFP transfected HeLa cells by fluorescence microscopy. We found three different abnormal cytochrome *c* distributions: (1) non-filamentous but condensed cytochrome *c* labeling, with normal round nuclei (Fig. 6a); (2) diffuse cytochrome *c* labeled and nuclei with a round shape and no condensed chromatin (Fig. 6b); (3) diffuse cytochrome *c* staining and condensed and/or fragmented nuclei (Fig. 6c). The quantification by immunofluorescence of the second staining pattern, as representative of proapoptotic cells showed that $30\pm8\%$ of the cells expressing NOA36-EGFP have proapoptotic features 48 h after transfection versus a $2\pm0.7\%$ of cells transfected with the empty vector ($P<0.05$) (Fig. 6d). Although these results indicated that transfecting NOA36-EGFP in cells induced cytochrome *c* release, it did not necessarily mean that NOA36-EGFP acts upstream of the mitochondrial membrane permeabilization, since cytochrome *c* release could also be due to a feedback mechanism of an event caused by NOA36-EGFP after mitochondrial outer membrane

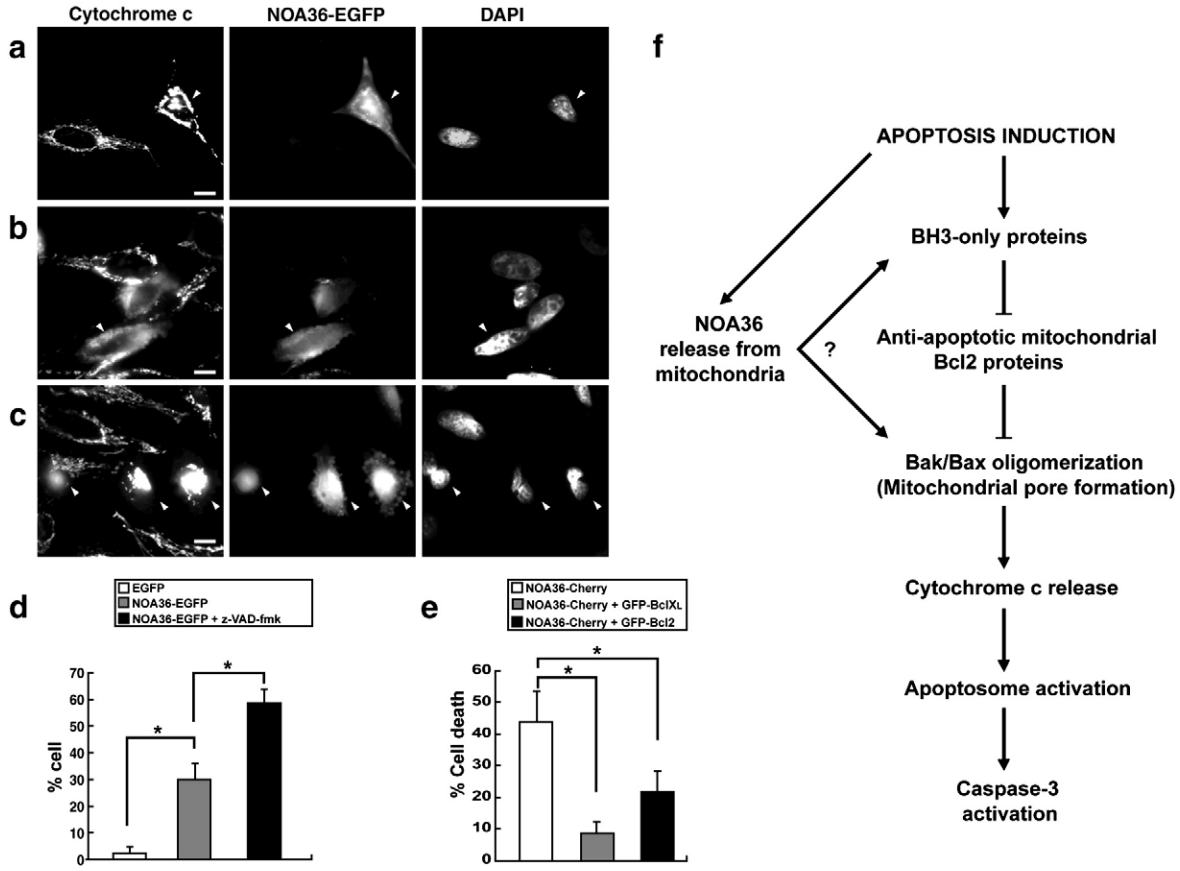

Fig. 6. NOA36 cytoplasmic expression induces cytochrome *c* release and its apoptotic effect is inhibited by Bcl-2 and Bcl-X_L overexpression. (a–c) Triple fluorescence with an anti-cytochrome *c* antibody (left panels), NOA36-EGFP (central panels) and DAPI chromatin staining (right panels). Three different abnormal cytochrome *c*–chromatin patterns (labeled with arrowheads) are detected in NOA36-EGFP transfected cells: (a) non-filamentous but condensed cytochrome *c* labeling and normal nuclei, (b) diffuse cytochrome *c*, nuclei with a round shape and no condensed chromatin, (c) diffuse cytochrome *c* staining and condensed/fragmented nuclei. Bar, 10 μm. (d) Bar diagram showing the percentage of cells showing pattern in (b) 48 h after transfection with EGFP (white bar), and NOA36-EGFP transfectants grown in a normal medium (grey bar) or in 100 μM z-VAD-fmk supplemented medium (black bar). (e) Bar diagram indicating the cell death rate induced by transfection with NOA36-Cherry (white bar) and co-transfected with GFP-Bcl-X_L (grey bar) or GFP-Bcl2 (black bar). (f) Schematic representation of the proposed role for NOA36 in the mitochondrial apoptotic pathway. After apoptosis induction, NOA36 is released from mitochondria. When located into cytoplasm, NOA36 acts upstream of cytochrome *c* to trigger the mitochondrial apoptotic pathway. The error bars in (d) and (e) represent standard deviation of the mean. Significant differences ($n=5$, $P<0.05$) are marked by asterisks (*).

permeabilization (MOMP). To evaluate whether or not NOA36-EGFP acts upstream of the mitochondrial membrane permeabilization, we also examined cytochrome *c* release when the mitochondrial downstream pathway (caspases activation) was blocked by the pan caspase-inhibitors z-VAD-fmk in NOA36-EGFP transfected cells. We found that blocking downstream events to mitochondria permeabilization by inhibiting all the caspases activity there was no decrease in the proportion of cells with diffuse cytochrome *c* staining — as could be expected if NOA36-EGFP acted downstream MOMP; on the contrary, there was a remarkable increment (up to $58\pm9\%$) of this staining pattern ($P<0.05$) probably due to the accumulation of cells in which MOMP have already occurred but with no other apoptotic characteristics (i.e. nuclear fragmentation, blebbing cytoplasm, etc).

Another attribute of the apoptotic mitochondrial permeabilization is that it can be blocked by over-expression of antiapoptotic mitochondrial proteins like Bcl-2 and Bcl-X_L [32]. We analysed this feature by co-transfection of NOA36-Cherry and GFP-Bcl-2 or GFP-Bcl-X_L. In both cases, apoptosis was drastically reduced in double transfectants ($P<0.05$), although over-expression of Bcl-X_L was more efficient and almost completely avoided all the apoptotic activity of cytoplasmic NOA36-EGFP (Fig. 6e).

Altogether these data suggest that ectopic expression of cytoplasmic NOA36-EGFP causes a redistribution of cytochrome *c* from the mitochondria to the cytoplasm, upstream mitochondrial permeabilization to trigger the mitochondrial apoptotic pathway.

5. Discussion

Elucidating the function of the intracellular signalling molecules that mediate apoptosis will provide valuable insights into the mechanisms of cell death and possible routes for treatment of human diseases in which apoptosis regulation is impaired. Here we characterize the proapoptotic activity of NOA36, a protein reported as a nucleolar autoantigen 10 years ago but whose function remained unknown. Our results demonstrate that the conserved NOA36 protein is also localized in the mitochondria, very likely in association with the cytosolic side of the outer membrane. Relatively little is known about the mechanism of insertion and assembly of outer membrane proteins (reviewed in ref. [35]). Like all known proteins located at the mitochondrial outer membrane, NOA36 do not contain a canonical cleavable N-terminal presequence, suggesting that it is likely bound to mitochondrial protein(s). Since NOA36 may be involved in MOMP, we also investigated whether it bound to anti-apoptotic Bcl-2 family members such as Bcl-2 or Bcl-X_L; however, GST pull-down and immunoprecipitation assays did not reveal direct interaction with these mitochondrial proteins (data not shown). Our aim in a future work is to study the interaction of NOA36 with others mitochondrial proteins by antibody arrays of apoptotic proteins and/or by yeast two hybrids.

We also show that NOA36 mitochondrial localization is dynamic, as occurs with certain proteins which are not permanently anchored

to the outer membrane but rather associate with the membrane in a dynamic manner. In this sense, proteins located at other cellular compartments can be also transported to the mitochondria. For instance, it has been shown that during apoptosis, Bad can direct p53 specifically to mitochondria [36].

Since the pioneering work of Wang and coworkers identified cytochrome *c* as a key component of the apoptosis pathway [17], mitochondria have been central to apoptosis research. Due to NOA36 mitochondrial localization, we considered a possible function for NOA36 in the programmed cell death process. Our results show that downregulation of NOA36 expression desensitizes HeLa cells to CPT, ETO and STS mediated apoptosis but not to the death receptors ligands anti-Fas antibody or TRAIL. The most evident apoptotic attenuation was found after treatment with topoisomerases inhibitors CPT and ETO, which generate nonrepairable protein-linked DNA double-strand breaks. These results are suggestive of a proapoptotic function of NOA36 linked to the mitochondrial death pathway and probably with a more specific role in the apoptosis induced by DNA damage. NOA36 is translocated from the mitochondria to the cytoplasm during apoptosis in HeLa cells and we found a high apoptosis-inducing activity when NOA36 is ectopically expressed in cytosol but not in the nucleoli. Although translocation of NOA36 to the cytoplasm was also found after TRAIL treatment, NOA36 seems to have a minor role in the apoptosis activated by extracellular signals, since downregulation of NOA36 has no effect in apoptosis induced by anti-Fas antibody or TRAIL.

The translocation of proapoptotic proteins like SMAC/DIABLO, ARTS and HtrA2/Omi from the mitochondria to the cytosol is a relevant feature in apoptosis activation. However, there are two important differences between these proteins and NOA36 proapoptotic activity. Firstly these proteins are located at the intermitochondrial membrane space, whereas NOA36 is located at the cytosolic side of the outer mitocondrial membrane. Secondly, whilst these mediators are liberated to the cytosol as a consequence of mitochondrial pore formation, our data would suggest that NOA36 could activate the apoptotic intrinsic pathway upstream of mitochondrial outer membrane permeabilization, since cytochrome *c* release – an event secondary to mitochondrial permeabilitation – can be detected in the cytoplasm in a significant proportion of transfected cells ectopically expressing cytoplasmic NOA36-EGFP. Nevertheless, to demonstrate that endogenous NOA36 is released upstream cytchrome *c* release, kinetic studies should be carried out with different apoptosis inductors. This will help us to definitely determine whether or not NOA36 is released from the mitochondria before cytochrome *c*. In this case, NOA36 could represent a new kind of mitochondrial proapoptotic protein with a possible role in upstream events to mitochondrial pore formation, either via activation of molecules involved in pore formation (Bax, Bak) or by activating one or more of the BH3-only proteins that eventually could cause pore formation and cytochrome *c* release (Fig. 6f).

The analysis of apoptosis induction of several NOA36 truncated proteins has revealed that a short amino acid sequence, with no significant homology with others proapoptotic domains, is the main responsible for the cell death inducing properties of NOA36. This sequence contains amino acids from 92 to 139 in the human protein and could form a Zn finger domain, with two C-X-X-C motives at C and N ends. This apoptotic activity in a protein containing (C-X-X-C) motives contrast with the fact that, many cellular protective proteins contain this motif in their active sites (e.g., thioredoxin, peroxiredoxin, protein disulfide, etc.).

In summary, our findings demonstrate that NOA36 is a mitochondrial protein located on the cytosolic side of the outer membrane that is released from mitochondria during apoptosis and becomes part of the machinery that brings about cell death. To our knowledge, this is the first evidence showing that NOA36 ha functional relevance within the cell. Its association with cell death makes this protein an interesting candidate to study in biological processes, where apoptosis is impaired. Further research will elucidate the molecular mechanism underlying the apoptotic activity of NOA36.

Acknowledgments

We would like to thank Dr. R.Y. Tsien for the Cherry DNA, Dr. R.J. Youle for the Bcl-2 and Bcl-XL constructs and Dr. M.M. Valdivia for the anti-H1 antibody. We also thank Antonio Astola for helping us in Western blotting quantification, F.J. Garcia-Cozar for helpful discussions and M. Dominguez for critical reading of the manuscript. We are grateful to Dr. C. Andoniadou for help editing this manuscript. This work was supported by a grant from 'Ministerio de Ciencia y Tecnologia' of Spain (SAF2003-06398).

Appendix A. Supplementary data

Supplementary data associated with this article can be found, in the online version, at doi:10.1016/j.bbamcr.2009.10.011.

References

[1] M.D. Jacobson, M. Weil, M.C. Raff, Programmed cell death in animal development, Cell 88 (1997) 347–354.
[2] G.I. Evan, K.H. Vousden, Proliferation, cell cycle and apoptosis in cancer, Nature 411 (2001) 342–348.
[3] D. Hanahan, R.A. Weinberg, The hallmarks of cancer, Cell 100 (2000) 57–70.
[4] G.S. Robertson, S.J. Crocker, D.W. Nicholson, J.B. Schulz, Neuroprotection by the inhibition of apoptosis, Brain Pathol. 10 (2000) 283–292.
[5] C.B. Thompson, Apoptosis in the pathogenesis and treatment of disease, Science 267 (1995) 1456–1462.
[6] Y. Shi, Mechanisms of caspase activation and inhibition during apoptosis, Mol. Cell 9 (2002) 459–470.
[7] S. Nagata, Apoptosis by death factor, Cell 88 (1997) 355–365.
[8] S. Wang, W.S. El Deiry, TRAIL and apoptosis induction by TNF-family death receptors, Oncogene 22 (2003) 8628–8633.
[9] D.R. Green, J.C. Reed, Mitochondria and apoptosis, Science 281 (1998) 1309–1312.
[10] S. Cory, J.M. Adams, The Bcl2 family: regulators of the cellular life-or-death switch, Nat. Rev., Cancer 2 (2002) 647–656.
[11] J. Pawlowski, A.S. Kraft, Bax-induced apoptotic cell death, Proc. Natl. Acad. Sci. U. S. A. 97 (2000) 529–531.
[12] J. Zha, H. Harada, E. Yang, J. Jockel, S.J. Korsmeyer, Serine phosphorylation of death agonist BAD in response to survival factor results in binding to 14-3-3 not BCL-X (L), Cell 87 (1996) 619–628.
[13] S. Desagher, A. Osen-Sand, A. Nichols, R. Eskes, S. Montessuit, S. Lauper, K. Maundrell, B. Antonsson, J.C. Martinou, Bid-induced conformational change of Bax is responsible for mitochondrial cytochrome *c* release during apoptosis, J. Cell Biol. 144 (1999) 891–901.
[14] L. O'Connor, A. Strasser, L.A. O'Reilly, G. Hausmann, J.M. Adams, S. Cory, D.C. Huang, Bim: a novel member of the Bcl-2 family that promotes apoptosis, EMBO J. 17 (1998) 384–395.
[15] H. Puthalakath, A. Strasser, Keeping killers on a tight leash: transcriptional and post-translational control of the pro-apoptotic activity of BH3-only proteins, Cell Death Differ. 9 (2002) 505–512.
[16] R.M. Kluck, E. Bossy-Wetzel, D.R. Green, D.D. Newmeyer, The release of cytochrome *c* from mitochondria: a primary site for Bcl-2 regulation of apoptosis, Science 275 (1997) 1132–1136.
[17] X. Liu, C.N. Kim, J. Yang, R. Jemmerson, X. Wang, Induction of apoptotic program in cell-free extracts: requirement for dATP and cytochrome *c*, Cell 86 (1996) 147–157.
[18] J. Yang, X. Liu, K. Bhalla, C.N. Kim, A.M. Ibrado, J. Cai, T.I. Peng, D.P. Jones, X. Wang, Prevention of apoptosis by Bcl-2: release of cytochrome *c* from mitochondria blocked, Science 275 (1997) 1129–1132.
[19] H. Zou, Y. Li, X. Liu, X. Wang, An APAF-1.cytochrome *c* multimeric complex is a functional apoptosome that activates procaspase-9, J. Biol. Chem. 274 (1999) 11549–11556.
[20] C. Du, M. Fang, Y. Li, L. Li, X. Wang, Smac, a mitochondrial protein that promotes cytochrome *c*-dependent caspase activation by eliminating IAP inhibition, Cell 102 (2000) 33–42.
[21] A.M. Verhagen, P.G. Ekert, M. Pakusch, J. Silke, L.M. Connolly, G.E. Reid, R.L. Moritz, R.J. Simpson, D.L. Vaux, Identification of DIABLO, a mammalian protein that promotes apoptosis by binding to and antagonizing IAP proteins, Cell 102 (2000) 43–53.
[22] R. Hegde, S.M. Srinivasula, Z. Zhang, R. Wassell, R. Mukattash, L. Cilenti, G. DuBois, Y. Lazebnik, A.S. Zervos, T. Fernandes-Alnemri, E.S. Alnemri, Identification of Omi/HtrA2 as a mitochondrial apoptotic serine protease that disrupts inhibitor of apoptosis protein-caspase interaction, J. Biol. Chem. 277 (2002) 432–438.
[23] Y. Suzuki, Y. Imai, H. Nakayama, K. Takahashi, K. Takio, R. Takahashi, A serine protease, HtrA2, is released from the mitochondria and interacts with XIAP, inducing cell death, Mol. Cell 8 (2001) 613–621.

[24] Y. Gottfried, A. Rotem, R. Lotan, H. Steller, S. Larisch, The mitochondrial ARTS protein promotes apoptosis through targeting XIAP, EMBO J. 23 (2004) 1627–1635.
[25] S.A. Susin, H.K. Lorenzo, N. Zamzami, I. Marzo, B.E. Snow, G.M. Brothers, J. Mangion, E. Jacotot, P. Costantini, M. Loeffler, N. Larochette, D.R. Goodlett, R. Aebersold, D.P. Siderovski, J.M. Penninger, G. Kroemer, Molecular characterization of mitochondrial apoptosis-inducing factor, Nature 397 (1999) 441–446.
[26] L.Y. Li, X. Luo, X. Wang, Endonuclease G is an apoptotic DNase when released from mitochondria, Nature 412 (2001) 95–99.
[27] J. Parrish, L. Li, K. Klotz, D. Ledwich, X. Wang, D. Xue, Mitochondrial endonuclease G is important for apoptosis in *C. elegans*, Nature 412 (2001) 90–94.
[28] E.M. Tan, Y. Muro, K.M. Pollard, Autoantibody-defined epitopes on nuclear antigens are conserved, conformation-dependent and active site regions, Clin. Exp. Rheumatol. 12 (Suppl. 11) (1994) S27–S31.
[29] J. Bolivar, I. Diaz, C. Iglesias, M.M. Valdivia, Molecular cloning of a zinc finger autoantigen transiently associated with interphase nucleolus and mitotic centromeres and midbodies. Orthologous proteins with nine CXXC motifs highly conserved from nematodes to humans, J. Biol. Chem. 274 (1999) 36456–36464.
[30] J. Bolivar, F.J. Garcia-Cozar, A. Astola, C. Iglesias, C. Pendon, M.M. Valdivia, Genomic structure and chromosome location of the human gene encoding the zinc finger autoantigen ZNF330, Cytogenet. Cell Genet. 93 (2001) 234–238.
[31] J. Rush, A. Moritz, K.A. Lee, A. Guo, V.L. Goss, E.J. Spek, H. Zhang, X.M. Zha, R.D. Polakiewicz, M.J. Comb, Immunoaffinity profiling of tyrosine phosphorylation in cancer cells, Nat. Biotechnol. 23 (2005) 94–101.
[32] Y. Jan, M. Matter, J.T. Pai, Y.L. Chen, J. Pilch, M. Komatsu, E. Ong, M. Fukuda, E. Ruoslahti, A mitochondrial protein, Bit1, mediates apoptosis regulated by integrins and Groucho/TLE corepressors, Cell 116 (2004) 751–762.
[33] N.C. Shaner, R.E. Campbell, P.A. Steinbach, B.N. Giepmans, A.E. Palmer, R.Y. Tsien, Improved monomeric red, orange and yellow fluorescent proteins derived from Discosoma sp. red fluorescent protein, Nat. Biotechnol. 22 (2004) 1567–1572.
[34] H. Zhu, H.O. Fearnhead, G.M. Cohen, An ICE-like protease is a common mediator of apoptosis induced by diverse stimuli in human monocytic THP.1 cells, FEBS Lett. 374 (1995) 303–308.
[35] D.M. Walther, D. Rapaport, Biogenesis of mitochondrial outer membrane proteins, Biochim. Biophys. Acta 1793 (2009) 42–51.
[36] P. Jiang, W. Du, K. Heese, M. Wu, The Bad guy cooperates with good cop p53: Bad is transcriptionally up-regulated by p53 and forms a Bad/p53 complex at the mitochondria to induce apoptosis, Mol. Cell. Biol. 26 (2006) 9071–9082.